Tetraspanin CD82 Organizes Dectin-1 into Signaling Domains to Mediate Cellular Responses to Candida albicans

Tam, Jenny M; Reedy, Jennifer L; Lukason, Daniel P; Kuna, Sunnie G; Acharya, Mridu; Khan, Nida S; Negoro, Paige E; Xu, Shuying; Ward, Rebecca A; Feldman, Michael B

Published in:
Journal of Immunology

DOI:
10.4049/jimmunol.1801384

The Journal of Immunology

Tetraspanin CD82 Organizes Dectin-1 into Signaling Domains to Mediate Cellular Responses to *Candida albicans*

Jenny M. Tam, Jennifer L. Reedy, Daniel P. Lukason, Sunnie G. Kuna, Mridu Acharya, Nida S. Khan, Paige E. Negoro, Shuying Xu, Rebecca A. Ward, Michael B. Feldman, Richard A. Dutko, Jane B. Jeffery, Anna Sokolovska, Carl N. Wivagg, Kara G. Lassen, François Le Naour, Vasiliki Matzaraki, Ethan C. Garner, Ramnik J. Xavier, Vinod Kumar, Frank L. van de Veerdonk, Mihai G. Netea, Cindy K. Miranti, Michael K. Mansour and Jatin M. Vyas

J Immunol 2019; 202:3256-3266; Prepublished online 22 April 2019;
doi: 10.4049/jimmunol.1801384
http://www.jimmunol.org/content/202/11/3256

The Journal of Immunology is published twice each month by
The American Association of Immunologists, Inc.,
1451 Rockville Pike, Suite 650, Rockville, MD 20852

Print ISSN: 0022-1767 Online ISSN: 1550-6606.

Tetraspanin CD82 Organizes Dectin-1 into Signaling Domains to Mediate Cellular Responses to *Candida albicans*

Jenny M. Tam,*,[1] Jennifer L. Reedy,*,[1] Daniel P. Lukason,* Sunnie G. Kuna,* Mridu Acharya,†,‡ Nida S. Khan,*,§,¶ Paige E. Negoro,* Shuying Xu,* Rebecca A. Ward,* Michael B. Feldman,¶,‖ Richard A. Dutko,* Jane B. Jeffery,* Anna Sokolovska,# Carl N. Wivagg,¶ Kara G. Lassen,,†† François Le Naour,‡‡ Vasiliki Matzaraki,§§ Ethan C. Garner,¶¶ Ramnik J. Xavier,¶,**,‖‖ Vinod Kumar,§§ Frank L. van de Veerdonk,§§ Mihai G. Netea,§§ Cindy K. Miranti,## Michael K. Mansour,*,¶ and Jatin M. Vyas*,¶**

Tetraspanins are a family of proteins possessing four transmembrane domains that help in lateral organization of plasma membrane proteins. These proteins interact with each other as well as other receptors and signaling proteins, resulting in functional complexes called "tetraspanin microdomains." Tetraspanins, including CD82, play an essential role in the pathogenesis of fungal infections. Dectin-1, a receptor for the fungal cell wall carbohydrate β-1,3-glucan, is vital to host defense against fungal infections. The current study identifies a novel association between tetraspanin CD82 and Dectin-1 on the plasma membrane of *Candida albicans*–containing phagosomes independent of phagocytic ability. Deletion of CD82 in mice resulted in diminished fungicidal activity, increased *C. albicans* viability within macrophages, and decreased cytokine production (TNF-α, IL-1β) at both mRNA and protein level in macrophages. Additionally, CD82 organized Dectin-1 clustering in the phagocytic cup. Deletion of CD82 modulates Dectin-1 signaling, resulting in a reduction of Src and Syk phosphorylation and reactive oxygen species production. CD82 knockout mice were more susceptible to *C. albicans* as compared with wild-type mice. Furthermore, patient *C. albicans*–induced cytokine production was influenced by two human CD82 single nucleotide polymorphisms, whereas an additional CD82 single nucleotide polymorphism increased the risk for candidemia independent of cytokine production. Together, these data demonstrate that CD82 organizes the proper assembly of Dectin-1 signaling machinery in response to *C. albicans*. *The Journal of Immunology*, 2019, 202: 3256–3266.

Invasive fungal infections are a major cause of morbidity and mortality worldwide, particularly among patients with immunodeficiency or alterations in host barrier defenses (1–3). The most prevalent fungal pathogen, *Candida albicans,* causes a wide spectrum of clinical disease ranging from mucocutaneous infections of the gastrointestinal tract and vagina to life-threatening disseminated infections (4, 5). *C. albicans* is the fourth leading cause of nosocomial-acquired blood stream infections, and even with the appropriate antifungal therapy, mortality rates remain at 30–50% (6, 7). This unacceptably high mortality rate highlights the limitations of our current antifungal armamentarium and underscores the need to understand better immune responses to *C. albicans* to develop new therapeutic approaches.

Tetraspanins, a conserved family of integral membrane proteins, play a significant role in the pathogenesis of infections (8). Tetraspanins are expressed on most cell types and regulate a diverse

*Division of Infectious Diseases, Department of Medicine, Massachusetts General Hospital, Boston, MA 02114; †Immunology Program, Benaroya Research Institute, Seattle, WA 98101; ‡Center for Immunity and Immunotherapies, Seattle Children's Research Institute, Seattle, WA 98101; §Biomedical Engineering and Biotechnology, University of Massachusetts Medical School, Worcester, MA 01655; ¶Department of Medicine, Harvard Medical School, Boston, MA 02115; ‖Pulmonary and Critical Care Medicine, Department of Medicine, Massachusetts General Hospital, Boston, MA 02114; #Department of Developmental Immunology, Massachusetts General Hospital, Boston, MA 02114; **Broad Institute of Harvard and MIT, Cambridge, MA 02142; ††Center for Computational and Integrative Biology, Massachusetts General Hospital, Boston, MA 02114; ‡‡Inserm, Unité 1193, 94800 Villejuif, France; §§Department of Internal Medicine and Radboud Center for Infectious Diseases, Radboud University Medical Center, 6500 HB Nijmegen, the Netherlands; ¶¶Center for Systems Biology, Harvard University, Boston, MA 02115; ‖‖Gastrointestinal Unit/Center for the Study of Inflammatory Bowel Disease, Massachusetts General Hospital, Boston, MA 02114; and ##Department of Cellular and Molecular Medicine, University of Arizona Health Sciences, Tucson, AZ 85724

[1]J.M.T. and J.L.R. equal contribution to manuscript.

ORCIDs: 0000-0003-1829-5735 (D.P.L.); 0000-0002-5448-8289 (N.S.K.); 0000-0001-6752-5600 (R.A.W.); 0000-0001-7023-461X (K.G.L.); 0000-0002-5852-6801 (V.M.); 0000-0003-0141-3555 (E.C.G.); 0000-0002-9985-9565 (J.M.V.).

Received for publication October 15, 2018. Accepted for publication March 26, 2019.

This work was supported by National Institutes of Health Grants 5R01 AI092084 and 1R01 AI097519 (to J.M.V.), 1R01 AI132638 (to M.K.M.), and T32 A1007061-35 (to J.L.R.), a KL2/Catalyst Medical Research Investigator Training award (an appointed KL2 award) from Harvard Catalyst | The Harvard Clinical Translational Science Center (National Center for Research Resources and the National Center for Advancing Translational Sciences, National Institutes of Health, Award KL2 TR001100 [to J.L.R.]), and National Institutes of Health Training Grant T32 HL116275 (to M.B.F.). M.G.N. was supported by a Spinoza Prize from the Netherlands Organization for Scientific Research. The content is solely the responsibility of the authors and does not necessarily represent the official views of Harvard Catalyst, Harvard University and its affiliated academic healthcare centers, or the National Institutes of Health.

Address correspondence and reprint requests to Dr. Jatin M. Vyas, Division of Infectious Diseases, Department of Medicine, Massachusetts General Hospital, 55 Fruit Street, Boston, MA 02114. E-mail address: jvyas@mgh.harvard.edu

The online version of this article contains supplemental material.

Abbreviations used in this article: BMDM, bone marrow–derived macrophage; co-IP, coimmunoprecipitation/coimmunoprecipitated; FLP, fungal-like particle; HKCA, heat-killed *C. albicans*; MGH, Massachusetts General Hospital; MOI, multiplicity of infection; PLA, proximity ligation assay; PRR, pattern recognition receptor; ROS, reactive oxygen species; SNP, single nucleotide polymorphism; STORM, stochastic optical reconstruction microscopy; Syk, spleen tyrosine kinase; TEM, tetraspanin-enriched microdomain; WT, wild-type; YPD, yeast extract peptone dextrose.

range of cellular functions, including cell morphology, invasion, motility, fusion, and signaling. Tetraspanins contain four transmembrane domains, a short intracellular amino and carboxy terminus, and two extracellular loops of unequal sizes (9, 10). Furthermore, they possess multiple conserved cysteine residues, a conserved CCG motif in the larger extracellular loop, and conserved palmitoylation sites (11, 12). Tetraspanins are located on endosomal membranes and interact with various proteins to establish functional multimeric complexes known as tetraspanin-enriched microdomains (TEMs) (13). The formation of TEMs within the cell membrane and intracellular vesicles facilitates the formation of functional protein complexes, enhancing signaling and other cellular functions. Defining the unique function of individual tetraspanins remains challenging because of a high degree of functional redundancy, lack of intrinsic tetraspanin catalytic domains, and insufficient tools (e.g., Abs).

The tetraspanin CD82, also known as Kai1, is involved in regulating cancer progression and immunity (14, 15). Downregulation of CD82 is associated with poor prognosis and tumor metastasis in multiple solid organ malignancies, including breast, colon, lung, ovarian, and pancreatic cancer (14, 16–20). In addition, CD82 regulates several processes, including cell adhesion, motility, and aggregation. At least 20 different tetraspanins, including CD82, are expressed on the surface of immune cells. Several of these tetraspanins (CD9, CD37, CD63, and CD81) interact with pattern recognition receptors (PRRs), such as C-type lectin receptors, TLRs, scavenger receptors, and Fc receptors (8, 9). In dendritic cells, cell surface expression of CD82 is upregulated upon activation and associates with class II MHC (21) as well as other components of the Ag-processing and presentation complex (22, 23). Interestingly, both macrophages and dendritic cells specifically recruit CD82 to phagosomes upon phagocytosis of various fungi, such as *Aspergillus fumigatus, Cryptococcus neoformans,* and *C. albicans* (24). However, the mechanism of CD82 in the innate immune response to fungal infections is poorly understood.

Dectin-1, a C-type lectin receptor, is expressed on the surface of innate immune cells, including macrophages and dendritic cells (25–27). Furthermore, Dectin-1 recognizes β-1,3-glucan, a fungal carbohydrate and component of the cell wall (28). Dectin-1 is critical for host defense against *C. albicans*, as demonstrated by increased susceptibility to *Candida* infections in both mice and humans lacking functional Dectin-1 (29, 30). Activation of Dectin-1 triggers phagocytosis, cytokine secretion, and reactive oxygen species (ROS) production that are all critical for anti-*Candida* defense (31, 32). Although Dectin-1 can bind both soluble and particulate β-1,3-glucan because of its ability to promote receptor clustering into "phagocytic synapses," only the particulate form of β-1,3-glucan can trigger Dectin-1–mediated signaling (33). Clustering of Dectin-1 receptors leads to activation of Src kinase, phosphorylation of the hemi-ITAM within the cytosolic tail of Dectin-1, and subsequent recruitment and activation of spleen tyrosine kinase (Syk) (34, 35). Additionally, Dectin-1 is known to interact with the tetraspanins CD37 and CD63 (36–38). Deficiency of CD37 leads to decreased Dectin-1 cell surface localization and significantly enhances Dectin-1–mediated IL-6 production (37).

Because CD82 is recruited to fungal phagosomes, we sought to define the role of CD82 in antifungal immune responses. We demonstrate that CD82 is required for generation of a proinflammatory cytokine response to *C. albicans* in macrophages. CD82 knockout ($CD82^{-/-}$) macrophages produce less TNF-α and IL-1β in response to *C. albicans* and are impaired in their ability to control *C. albicans* growth. Proteomic analysis of phagosomes containing chemically defined fungal-like particles (FLPs; purified fungal cell wall carbohydrate Ags covalently attached to polystyrene beads) revealed that CD82 associates with β-1,3-glucan and mannan containing phagosomes, suggesting interaction with Dectin-1. Association of CD82 and Dectin-1 on the fungal phagosome was confirmed using fluorescent microscopy, coimmunoprecipitation (co-IP), and proximity ligation assay (PLA). Using β-1,3-glucan FLPs that specifically stimulate Dectin-1, we demonstrate that the absence of CD82 impairs Dectin-1–mediated Syk and Src activation as well as ROS production. We further demonstrate by stochastic optical reconstruction microscopy (STORM) superresolution microscopy that CD82 regulates clustering of Dectin-1 at the phagocytic synapse and the absence of CD82 impairs Dectin-1 clustering. Additionally, mice lacking CD82 have increased susceptibility to *C. albicans*, further highlighting the importance of CD82. Lastly, human whole blood or PBMC samples showed two single nucleotide polymorphisms (SNPs) in CD82 which affected cytokine production and one additional CD82 SNP that increased the risk for candidemia without affecting cytokine production. Taken together, our results demonstrate a mechanistic role for CD82 in antifungal immune responses in macrophages by organizing the membrane to promote clustering of Dectin-1 into signaling domains.

Materials and Methods

Animals

Mice were maintained in specific pathogen–free facilities at Massachusetts General Hospital (MGH; Boston, MA). Macrophages were isolated from approximately equal numbers of both male and female mice between 6 and 8 wk of age. Primary macrophages were isolated from wild-type (WT) C57BL/6 mice (The Jackson Laboratory, Bar Harbor, ME), $CD82^{-/-}$ mice, and Dectin-$1^{-/-}$ mice. $CD82^{-/-}$ mice were a gift from Cindy Miranti, PhD (University of Arizona Health Sciences, Tucson, AZ), and the Dectin-$1^{-/-}$ mice were gifted by G. Brown, PhD (University of Aberdeen, Aberdeen, U.K.). All knockout mice were on a C57BL/6 background. All animal studies were conducted under protocols approved by the Institutional Animal Care and Use Committee Subcommittee on Research Animal Care at MGH.

Cell lines, viral transduction, and cell culture

The following cell lines were used: immortalized bone marrow–derived macrophages (BMDMs) from C57BL/6 (gifted by D. Golenbock, MD, University of Massachusetts Medical School, Worcester, MA), $CD82^{-/-}$ and Dectin-$1^{-/-}$ mice (gift from S. Levitz, MD, University of Massachusetts Medical School). Immortalized macrophages were generated using a J2 recombinant retrovirus with v-*myc* and v-*raf(mil)* oncogenes (39).

Cells were cultured in RPMI–GlutaMax (Life Technologies, Carlsbad, CA) containing 10% heat-inactivated FBS (HyClone, Logan, UT), 1% penicillin/streptomycin, 1% HEPES buffer, and 50 μM of 2-ME (RPMI 1640 complete media). Puromycin was added to a final concentration 5 μg/ml for selection of transduced cell lines. BMDM cell culture was adapted with the following modifications: cells were grown in media containing 20 ng/ml M-CSF (PeproTech, Rocky Hill, NJ) for 7 d in a tissue culture–treated plate with a 10-cm diameter. *C. albicans* (strain SC5314; American Type Culture Collection, Manassas, VA) was grown in yeast extract peptone dextrose (YPD) media (Sigma-Aldrich, St. Louis, MO) overnight in an orbital shaker at 30°C. The next morning, yeast was washed twice in sterile PBS and heat killed at 95°C for 30 min.

GFP–Dectin-1 (gifted by D. Underhill, PhD, Cedars-Sinai Medical Center, Los Angeles, CA) and HA-CD82 were subcloned into pHAGE II vector, which is a fourth-generation lentiviral self-inactivating nonreplicative vector. Immortalized C57BL/6 macrophages were stably transduced with GFP–Dectin-1, HA-CD82, or both GFP–Dectin-1 and HA-CD82 using the pHAGE II vector. HEK293T cells were used to produce the lentivirus, as described previously (40).

ELISA and CFUs

Primary WT and $CD82^{-/-}$ macrophages were plated in tissue culture–treated 24-well plates (Greiner Bio-One, Monroe, NC) at a density of 5×10^5 cells per well. Macrophages were stimulated under four

conditions: 1) media only, 2) live *C. albicans* (multiplicity of infection [MOI] = 10), 3) heat-killed *C. albicans* (HKCA; E:T = 1:10), or 4) LPS (200 ng/ml). TNF-α and IL-1β expression in cell supernatants was determined by the BD CBA Flex Set per manufacturer's instructions (BD Biosciences, Franklin Lakes, NJ). For CFU determination, cells were stimulated for 4 h, washed three times with PBS, then lysed with 0.02% Triton X-100. Serial dilutions from each well were made in nanopure water and plated on YPD agar plates with ampicillin (5 μg/ml). CFU was determined manually after incubation for 24 h at 30°C. For the CFU studies, an unpaired Mann–Whitney *U* test was used to test statistical significance, using GraphPad Prism7 software (GraphPad Software, La Jolla, CA). ELISA studies used a two-way ANOVA to test for statistical significance [(WT versus CD82$^{-/-}$) × (unstimulated versus *C. albicans* versus LPS)]. Bonferroni posthoc test was used to compare means from significant ANOVAs. A p value <0.05 was considered significant.

PrestoBlue assay

The PrestoBlue assay kit (Thermo Fisher Scientific, Waltham, MA) was used to measure fungal viability in WT and CD82$^{-/-}$ macrophages, according to manufacturer's protocol. Cells were plated in triplicate in a 96-well plate at a density of 1×10^5 cells per well. WT and CD82$^{-/-}$ BMDM were stimulated with live *C. albicans* (MOI = 1) for 4 h. Cells were then lysed with NP-40 to liberate phagocytosed yeast cells and centrifuged at 1500 rpm for 5 min. After incubating the lysate with the PrestoBlue reagent (1:10) for 24 h at 30°C, fluorescence was measured using a SpectraMax i3x Multi-Mode Microplate Reader system (Molecular Devices, San Jose, CA). Statistical significance was examined by an unpaired Mann–Whitney *U* test using GraphPad Prism7 software (GraphPad Software). A p value <0.05 was considered significant.

Real-time and quantitative PCR

Gene expression of cytokines (TNF-α and IL-1β) was measured by isolating RNA using the QIAGEN RNeasy Mini Kit. RNA was converted to cDNA using a High Capacity cDNA Reverse Transcription Kit (Thermo Fisher Scientific, Rochester, NY). Primers were designed using Primer-BLAST Software (National Center for Biotechnology Information). PCR of the cDNA was carried out using a S1000 Thermal Cycler (Bio-Rad Laboratories). Quantitative PCR analysis of the cDNA was performed using iTaq Universal SYBR Green Supermix (Bio-Rad Laboratories). A reverse transcriptase–negative sample was included as a control for each experiment. A melting curve analysis was done to confirm the specificity of primers used. An unpaired *t* test was used to test statistical significance of mRNA levels using GraphPad Prism7 software (GraphPad Software). A p value <0.05 was considered significant.

Confocal microscopy

Macrophages were plated in Nunc Lab-Tek 8-well Chambered Coverglass (Thermo Fisher Scientific) and allowed to adhere overnight. The cells were stimulated with HKCA for 1 h (E:T = 1:5) and fixed with 4% PFA at room temperature. Saponin (0.2% saponin in PBS, 0.03 M sucrose, 1% BSA) was used to permeabilize cells for 10 min at room temperature. Nonspecific binding in cells was prevented by incubating with blocking buffer (2% goat serum, 1% BSA, 0.1% cold fish skin gelatin, 0.1% saponin, 0.05% Tween-20 in 0.01 M PBS, pH 7.2) for 1 h. Cells were incubated overnight at 4°C with specific primary Abs (GFP 1:300; Santa Cruz Biotechnology, Dallas, TX; HA 1:200; Cell Signaling, Danvers, MA) in dilution buffer (PBS, 0.05% Tween 20, 1% BSA, 0.1% saponin). Following three washes in dilution buffer, cells were incubated in secondary Abs (1:500) in dilution buffer for 1 h at room temperature. The Chambered Coverglass was then mounted with Vectashield Antifade Mounting Medium (Vector Laboratories, Burlingame, CA). Images were captured on a Nikon Inverted Microscope Eclipse Ti-E equipped with a CSU-X1 confocal spinning disk head (Yokogawa, Sugarland, TX), and a Coherent 4W continuous-wave laser (Coherent, Santa Clara, CA) excited the sample. A high-magnification, high-numerical aperture objective (Nikon, 100×, 1.49 numerical aperture, oil immersion) was used. Images were obtained using an EMCCD camera (Hamamatsu Photonics, Bridgewater, NJ). Image acquisition was performed using MetaMorph software (Molecular Devices, Downingtown, PA). Raw images were then cropped using Adobe Photoshop CS5 and assembled in Adobe Illustrator, version CS4 (Adobe Systems, San Jose, CA).

Phagosome isolation and proteomics

Phagosome isolation was adopted from previously described protocols (41). Briefly, macrophages were cultured in 10-cm plates at a density of 1×10^7 and were stimulated with FLPs (E:T = 25) for 45 min, followed by the addition of hypotonic lysis buffer (2 mM $MgCl_2$, 6 mM 2-ME, 10 mM HEPES) with protease inhibitor mixture (Roche, Indianapolis, IN). Next, cells were mechanically sheared by aspirating and ejecting cell suspension through a 1-cc syringe fitted with a 1/2-inch 26-gauge needle for 15 cycles. The addition of 62% (w/v) sucrose solution to a final of 40% was used to adjust the hypotonic buffer. A discontinuous gradient was then constructed in high-speed ultracentrifugation polyallomer tubes (Beckman Coulter, Brea, CA) overlaying 2 ml of 62%, lysed cell suspension at 40 (sample), 30, 25, and 10%. Sucrose gradients were then subjected to ultracentrifugation at 80,000 × g for 1 h at 4°C (SW-28 rotor, L8M Ultracentrifuge; Beckman Coulter, Brea, CA). Phagosomes were isolated at the interface of the 25/10% sucrose layers and washed in PBS.

For proteomics, GFP–Dectin-1 macrophages were incubated with FLPs at a ratio of 5:1 for 1 h. Macrophages were subjected to hypotonic lysis and mechanical shearing, as described above. The phagosomes were then washed in protein-free buffer, digested, and peptides were resolved by LTQ-Orbitrap Velos mass spectroscopy (42). High-field asymmetric waveform ion mobility spectrometry and photoionization is used to additionally capture hydrophobic proteins, classically missed with traditional ionizing techniques, increasing peptide yield by 30% (43). Proteomic data were compared with the mouse genome database. Analysis of the macrophage phagosomal protein repertoire comparing β-1,3-glucan to mannan FLP was annotated using Ingenuity software (QIAGEN Bioinformatics, Redwood City, CA).

Co-IP and Western blot

Cells were lysed with lysis buffer containing 1× Brij 58 and protease inhibitor mixture (Roche). Next, cell lysates were precleared with bare Protein G Sepharose beads. Following three washes in lysis buffer, the beads were placed in SDS-containing sample buffer with a reducing agent according to NuPage/Novex protocol. Samples were boiled for 10 min at 95°C, then separated on 4–15% NuPage Bis-Tris Gels (Life Technologies) and transferred to PVDF membranes (PerkinElmer, Waltham, MA). Nonspecific binding was blocked with 5% BSA in 0.1% PBS–Tween 20 (Sigma-Aldrich), followed by incubation with primary Abs bound to Dynabeads (Invitrogen, Carlsbad, CA) shaking overnight at 4°C. For co-IP data, anti–HA-HRP (Cell Signaling Technology) and anti-GFP–HRP (Santa Cruz Biotechnology) Abs (1:1000) were used. For Western blots, membranes were probed for either phosphorylated Src or phosphorylated Syk (Cell Signaling Technology). Membranes were then washed thoroughly with PBS–Tween (0.1%) and developed using ECL reagents (PerkinElmer) on Kodak BioMax XAR Film (Sigma-Aldrich). For reprobing, blots were stripped for 30 min at 37°C with Restore PLUS Stripping Buffer (Thermo Fisher Scientific). Actin was used as a loading control for all Western blots (Sigma-Aldrich). Films were evenly adjusted using Adobe Photoshop CS4 (Adobe Systems). ImageJ software was used to measure band intensity. Western blots were analyzed by a two-way ANOVA to test for statistical significance [(WT versus CD82$^{-/-}$) × (unstimulated versus live *C. albicans* versus HKCA)]. Bonferroni posthoc test was used to compare means from significant ANOVAs. A p value <0.05 was considered significant.

Lucigenin ECL assay for ROS

Macrophages from WT and CD82$^{-/-}$ mice were plated in a 96-well plate at a density of 5×10^4 cells per well. Twenty-four hours after cells were seeded, cells were placed on ice and washed in PBS three times. Cells were incubated on ice for 10 min in lucigenin solution (0.9 mM $CaCl_2$, 0.5 mM $MgCl_2$, 20 mM dextrose, and 20 μM lucigenin). Live *C. albicans* was added and briefly centrifuged to enable cell–ligand contact. The initial reading (0 min) was taken immediately following centrifugation. The plate was read every 10 min and placed into an incubator at 37°C between each measurement. All readings were taken using the SpectraMax i3x Multi-Mode Microplate Reader (Molecular Devices). An unpaired *t* test was used to test statistical significance in GraphPad Prism7. A p value <0.05 was considered significant.

Flow cytometry

Flow cytometry was used to analyze the expression of Dectin-1 on the cell surface of WT and CD82$^{-/-}$ macrophages. Macrophages were washed in PBS containing 2% BSA and stained with anti–Dectin-1 allophycocyanin-conjugated Ab (1 μg/ml; R&D Systems) or an irrelevant isotype (rat-IgG_{2a} Ab; eBioscience) for 1 h at room temperature. Surface fluorescence was assessed on a BD FACSAria II flow cytometer and cell sorter (Becton Dickinson, Franklin Lakes, NJ), and analysis was performed by FlowJo software (FlowJo, Ashland, OR).

PLA

A PLA was performed using the Duolink In Situ Red Starter Kit Mouse/Rabbit (Sigma-Aldrich). Immortalized macrophages expressing HA-CD82 and GFP–Dectin-1 were cultured on Nunc Lab-Tek Chambered Coverglass (Thermo Fisher Scientific) and stained as described above. The primary Abs used were anti-GFP and anti-HA. PLA probes Anti-Rabbit PLUS and Anti-Mouse MINUS were used with detection reagent red according to Duolink protocol. Cells were imaged using the confocal microscope as described above, and ImageJ was used to quantify the PLA signal. The number of positive foci were counted in 15 total cells in multiple (>5) fields of view per condition. An unpaired *t* test was used to test statistical significance in GraphPad Prism7. A p value <0.05 was considered significant.

STORM and quantification

Immortalized WT or CD82$^{-/-}$ macrophages overexpressing GFP–Dectin-1 were seeded on tissue culture–treated Chambered Coverglass (Thermo Fisher Scientific) and stimulated for 15 min with HKCA. The cells were then fixed with 4% PFA at room temperature and subjected to the STORM using the GFP-Booster, and anti-GFP Ab conjugated to the photo-switchable dye ATTO488 (ChromoTek, Hauppauge, NY). A Nikon N-STORM microscope was used to image samples at a 60× objective using the "Perfect Focus" system. Imaging was performed in an extracellular solution containing reducing and oxygen scavengers, as specified by dSTORM protocols (44). The fluorochromes were first converted to a photo-switchable state using 488 nm at 60 mW. Once the fluorochromes were converted into a desired density of single molecules per frame, they were imaged continuously at 10,000–30,000 frames. Localization was acquired using an Andor 512 × 512 back-thinned EMCCD and reconstructed with Nikon Elements Imaging Software with a 50-ms exposure time.

For cluster quantification, reconstructed STORM data were analyzed using Voronoi tessellation in SR-Tesseler software (45). Default parameters and a density factor of 1.3 were used. This method subdivides a superresolution image into polygons based on molecular local densities. Quantification was performed on six two-dimensional reconstructed images.

In vivo candidemia study

C. albicans was grown in YPD media with 100 μg/ml ampicillin overnight at 30°C in a shaker incubator at 250 rpm. Yeast was washed and resuspended at a concentration (500,000 yeast/ml) in ice-cold PBS. WT and CD82$^{-/-}$ mice were injected i.v. into the lateral tail vein with *C. albicans* (100,000 yeast). Following the *C. albicans* challenge, mice were monitored once daily for morbidity and mortality for up to 28 d. Mice displaying prespecified criteria for distress (inability to feed or drink, labored breathing, ruffled and/or matted fur, decreased activity, hunched posture, and shivering) were euthanized by CO_2 asphyxiation. All mouse experiments were done under protocols approved by the MGH Institutional Animal Care and Use Committee.

Identification of CD82 human polymorphisms

SNPs within the CD82 gene and cytokine quantitative trait loci were identified as previously described (46). Briefly, we extracted SNPs located within the CD82 gene (window size of ±250 kb around the gene) and tested for their effect on CD82 expression levels using HaploReg (47). We then extracted the association between CD82 SNPs and cytokine levels using previously published data from Human Functional Genomics Project (46). Association between CD82 SNPs and susceptibility to candidemia were extracted from previous candidemia genetic studies (48, 49).

Results

CD82 is required for control of C. albicans *and cytokine secretion in macrophages*

To determine the role of CD82 in the killing of *C. albicans,* primary BMDM from C57BL/6 WT and CD82$^{-/-}$ mice were stimulated with live *C. albicans* for 4 h. Macrophages were then lysed to release phagocytosed yeast and either plated on agar plates for a CFU assay or added to PrestoBlue solution with YPD for a viability assay for 24 h. There was a significant increase in fungal viability in the CD82$^{-/-}$ macrophages compared with WT macrophages as measured by CFU at MOI = 5 after stimulation (Fig. 1A). In addition to CFU, we investigated fungal viability by PrestoBlue assay to ensure we fully accounted for the hyphal transition of *C. albicans* in the growth assay. Fungal viability of *C. albicans* in WT and CD82$^{-/-}$ macrophages was measured using the PrestoBlue cell viability assay after stimulation with live *C. albicans* for 4 h. *C. albicans* from CD82$^{-/-}$ macrophages (MOI = 5) had higher fungal viability when compared with fungi from WT macrophages (Fig. 1B). These results indicate that CD82 enhances fungal killing in macrophages.

We sought to determine the role of CD82 in regulating cytokine production in response to *C. albicans* stimulation. Supernatants

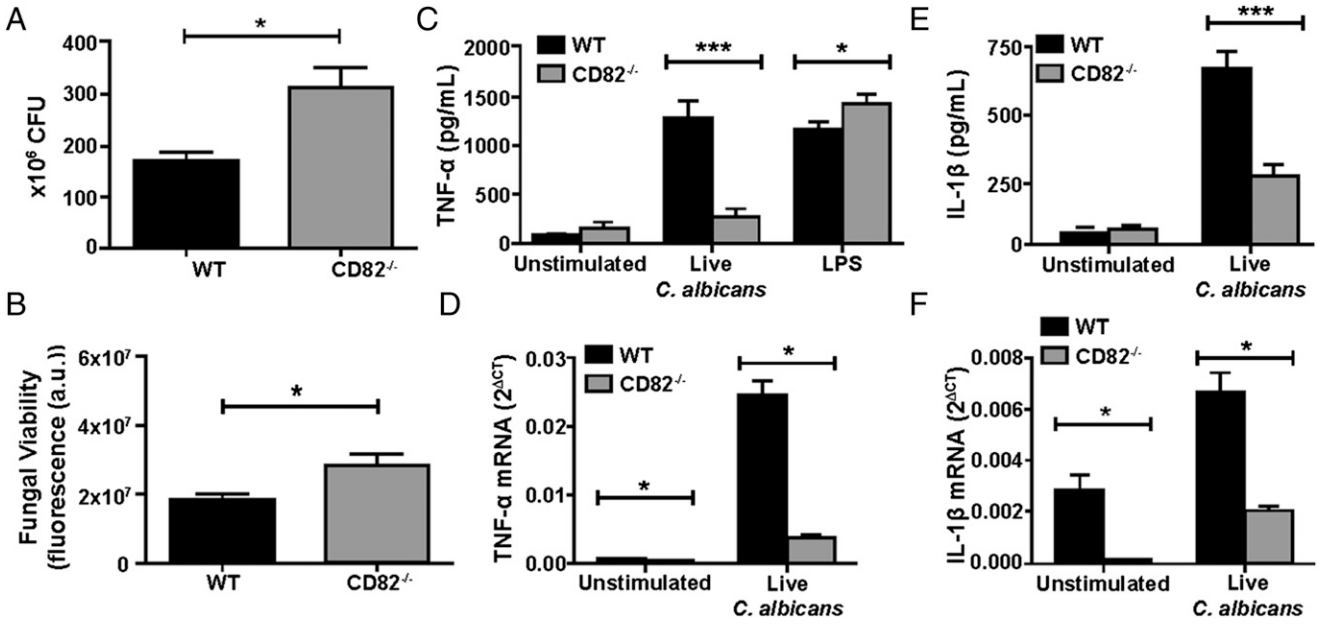

FIGURE 1. CD82 regulates fungal survival and cytokine production. CD82$^{-/-}$ macrophages have increased fungal viability compared with WT macrophages as measured by CFU (**A**) and PrestoBlue (**B**). Decreased TNF-α (**C**) and IL-1β production (**E**) was observed in CD82$^{-/-}$ macrophages (gray bar) compared with WT macrophages (black bar) upon *C. albicans* stimulation. CD82$^{-/-}$ macrophages had reduced levels of TNF-α (**D**) and IL-1β (**F**) mRNA compared with WT macrophages (n = 3). *$p < 0.05$, ***$p < 0.01$ versus WT.

from *C. albicans*–stimulated primary and immortalized WT and CD82$^{-/-}$ macrophages (MOI = 5) were analyzed for TNF-α and IL-1β cytokine production. Macrophages stimulated with live *C. albicans* showed reduced production of TNF-α and IL-1β in the absence of CD82 as compared with WT (Fig. 1C, 1E). Similarly, primary CD82$^{-/-}$ macrophages stimulated with live *C. albicans* (MOI = 10) showed decreased mRNA expression compared with WT macrophages (Fig. 1D, 1F). To determine if this change in cytokine production was specific to fungal-derived ligands, we stimulated cells with LPS and measured TNF-α production by ELISA. These data showed comparable TNF-α levels in CD82-deficient mice as compared with WT (Fig. 1C). Together, these data suggest that CD82 is required for cytokine production and gene expression in response to *C. albicans*.

CD82 associates with Dectin-1 on the fungal phagosome

To determine whether CD82 closely associates with Dectin-1 on the fungal phagosome, we conducted a proteomic analysis of membrane proteins associated with either β-1,3-glucan or mannan FLP-containing phagosomes. Analysis shows that of the 1482 proteins identified, 775 were shared between β-1,3-glucan beads and mannan FLPs. A total of 354 proteins were uniquely associated with β-1,3-glucan, and 353 proteins were associated with mannan FLPs. CD82 was associated with both β-1,3-glucan and mannan FLP-containing phagosomes (Fig. 2A).

To confirm CD82 recruitment to β-1,3-glucan phagosomes, we stimulated macrophages overexpressing CD82–mRFP1 and GFP–Dectin-1 with β-1,3-glucan FLP and performed phagosome isolation (50, 51). Phagosomes were separated by $NaDodSO_4$–PAGE followed by immunoblotting for RFP. The corresponding band is to CD82–RFP (Fig. 2B). To visualize the association of Dectin-1 and CD82 in the phagosome, we stimulated immortalized macrophages overexpressing CD82–mRFP1 and GFP–Dectin-1 with HKCA for 1 h (E:T = 5:1). Confocal microscopy showed that Dectin-1 was recruited to the *C. albicans* phagosome, as we have shown previously (50). Interestingly, we also see recruitment of CD82 to the fungal phagosome in addition to Dectin-1. Furthermore, we observed colocalization of Dectin-1 and CD82 on *C. albicans*–containing phagosomes (Fig. 2C).

CD82 associates with Dectin-1

Because CD82 and Dectin-1 associate on the fungal phagosome, we next investigated whether Dectin-1 and CD82 associate on the plasma membrane at a resting state. We first performed co-IP experiments using immortalized macrophages. Because the strength and nature of the tetraspanin–protein interaction is determined by the degree of resistance to detergent conditions (52), co-IP experiments were done under mild (Brij 58) and strong (Triton X-100) lysis conditions. Interactions that are stable in 1% Triton X-100 buffers are usually considered to be strong and direct, whereas stability in only mild detergents indicates indirect interactions (53). Interactions between CD82 and Dectin-1 were only observed under Brij 58 lysis conditions but not under Triton X-100 conditions, indicating an indirect interaction (data not shown). To determine specificity of co-IP lysis conditions, macrophages were modified to overexpress CD82 and/or Dectin-1 as follows: 1) WT, 2) expression of GFP–Dectin-1 only, 3) expression of HA-CD82 only, and 4) expression of both GFP–Dectin-1

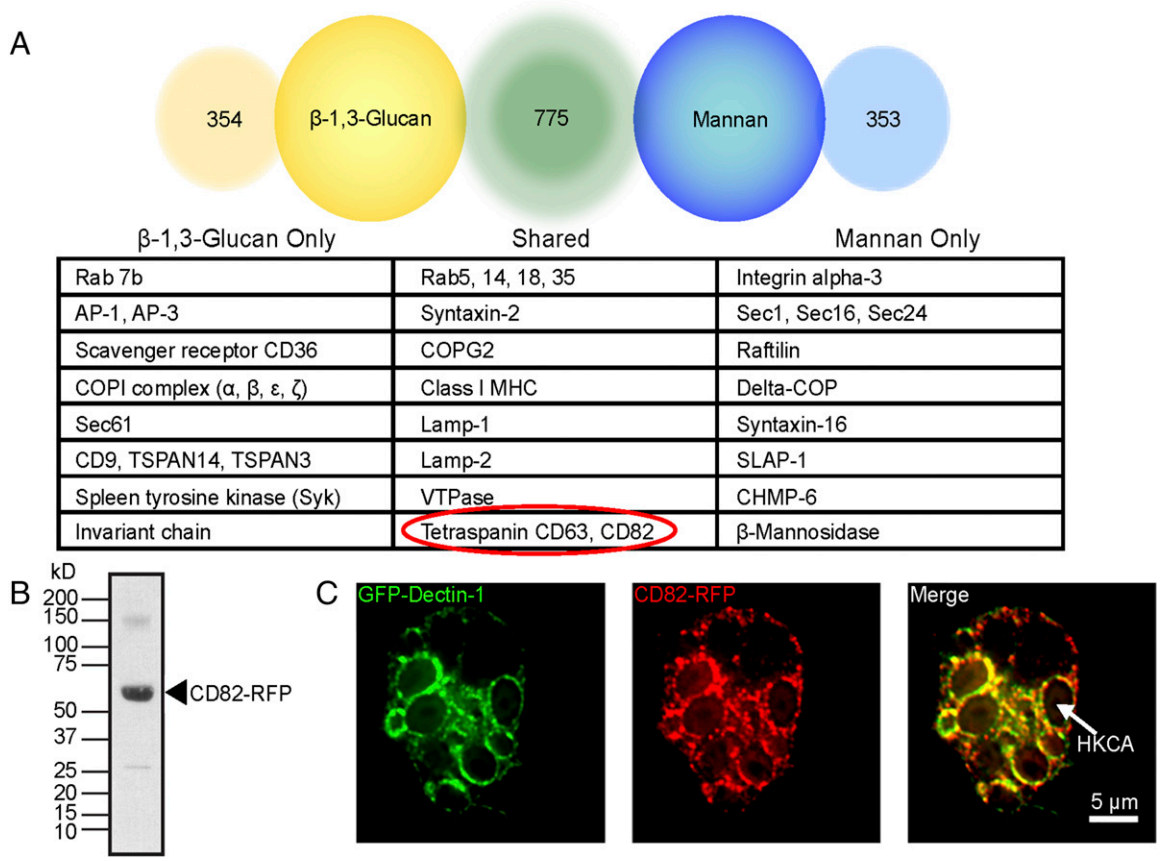

FIGURE 2. Dectin-1 and CD82 associate on the fungal phagosome. (**A**) CD82 is shown in a partial list of proteomic hits from macrophages stimulated by either β-1,3-glucan or mannan FLPs. (**B**) Immunoblot of purified β-1,3-glucan FLP-containing phagosomes confirms CD82–mRFP1 localization to the phagosome using an anti-RFP Ab. (**C**) Colocalization of GFP–Dectin-1 and CD82–mRFP1 was observed by confocal microscopy in immortalized macrophages. Scale bar, 5 μm. Arrow indicates a phagosome containing HKCA.

and HA-CD82. Macrophages were unstimulated, stimulated by live *C. albicans*, or stimulated by HKCA. HKCA was used for our molecular studies because heat-killed yeast has higher β-1,3-glucan exposure on the cell wall compared with live *C. albicans* (54). In macrophages lacking GFP–Dectin-1 and/or HA-CD82, no co-IP band was observed when stimulated with live or HKCA. Under all three stimulation conditions, macrophages expressing both Dectin-1 and CD82 showed a positive co-IP band. Importantly, GFP–Dectin-1 could be co-IP with HA-CD82 (data not shown), showing that the co-IP between CD82 and Dectin-1 worked in both directions (Fig. 3A).

To confirm the association of Dectin-1 and CD82 observed by confocal microscopy and co-IP, we next used PLA, a PCR-based method that allows quantification of sites of close interaction between proteins by microscopy (55). Following 15 min of stimulation with HKCA, PLA showed association between CD82 and Dectin-1 (Fig. 3B). However, no association was seen by PLA in a resting state, unstimulated by *C. albicans*, which suggests >40 nm separates CD82 and Dectin-1 in resting macrophages. The increased PLA signal in stimulated macrophages suggests that CD82 and Dectin-1 become more closely associated (<40 nm) when activated by *C. albicans* (Fig. 3C). Together, these biochemical and microscopy approaches strongly suggest an indirect association between the tetraspanin CD82 and Dectin-1 in macrophages.

CD82 is required for downstream Dectin-1 signaling

To understand the effects of CD82 association with Dectin-1, we analyzed downstream components of the Dectin-1 signaling pathway in CD82$^{-/-}$ macrophages. Upon stimulation of Dectin-1, Src-mediated signaling occurs in response to β-1,3-glucan binding. The ITAM motif of Dectin-1 is phosphorylated by Src kinase, resulting in the recruitment of Syk and subsequent ROS production (32, 34). Phosphorylation of Src family kinases and Syk was measured in immortalized WT and CD82$^{-/-}$ macrophages simulated with either live or HKCA. Phosphorylation of both Src family kinases and Syk started to occur 30 min after stimulation and further increased at 60 min (Fig. 4A, 4B). In sharp contrast, CD82$^{-/-}$ macrophages showed little phosphorylation of Src family kinases and Syk at similar time points compared with WT macrophages. The failure of sustained Src and Syk phosphorylation in macrophages lacking CD82 corresponds with reduced ROS production (Fig. 4C). Together, these observations show that CD82 is required for Dectin-1 signaling pathway and subsequent ROS production.

Comparable Dectin-1 expression and phagocytic uptake in WT and CD82$^{-/-}$ macrophages

Because CD82 appears to play a role in the Dectin-1 signaling cascade upon stimulation by *C. albicans*, we next wanted to determine whether CD82$^{-/-}$ macrophages influenced Dectin-1 surface expression or phagocytic capacity. Analysis of Dectin-1 surface expression from primary macrophages by flow cytometry showed similar expression of Dectin-1 in CD82$^{-/-}$ macrophages compared with the WT control (Fig. 5A). To determine whether defects in Dectin-1 signaling could be due to defective phagocytosis in CD82$^{-/-}$ macrophages, we compared HKCA labeled with Alexa Fluor 647 phagocytosed by WT and CD82$^{-/-}$ macrophages. After stimulation of macrophages by HKCA, no difference was observed in phagocytic uptake between WT and CD82-deficient macrophages (Fig. 5B). As a control, we compared phagocytosis in macrophages lacking Dectin-1 compared with WT cells. As expected, Dectin-1$^{-/-}$ macrophages did show a lower phagocytic uptake of HKCA compared with the WT cells (Fig. 5B, white bar). These results show that the loss of Src and Syk phosphorylation, as well as ROS production, is not because of any differences in Dectin-1 expression or phagocytic uptake of *C. albicans*.

CD82 licenses Dectin-1 clustering in the phagocytic synapse

Because we observed an association between CD82 and Dectin-1, we next investigated how CD82 organizes Dectin-1 in TEMs on the plasma membrane. Whereas we can visualize CD82 and Dectin-1 on the macrophage plasma membrane using spinning disk confocal microscopy, we were unable to analyze Dectin-1 clustering because of limitations of conventional light microscopy. Individual Dectin-1 clusters cannot be discerned in the phagocytic cup using standard epifluorescence imaging (Supplemental Fig. 1A). However, when the same cells are imaged at a greater resolution by STORM,

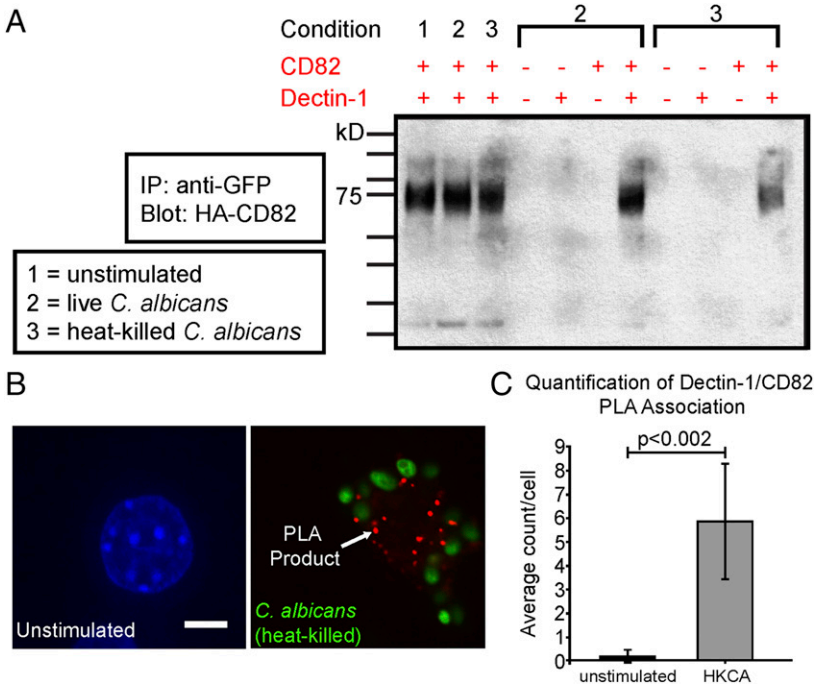

FIGURE 3. Dectin-1 and CD82 interact in macrophages. (**A**) Dectin-1 and CD82 associate with each other as seen by co-IP of immortalized macrophages expressing HA–CD82 and GFP–Dectin-1 in resting macrophages and in cells stimulated with live and HKCA. (**B**) Representative images of the association between Dectin-1 and CD82 in stimulated macrophages expressing GFP–Dectin-1 and HA-CD82 as measured by PLA. Association was observed in macrophages stimulated by HKCA. Size bar, 5 μm. (**C**) Quantification of Dectin-1/CD82 PLA association confirms the number of positive colocalizations per cell in unstimulated versus stimulated macrophages. Data are from analysis of at least 20 cells per condition.

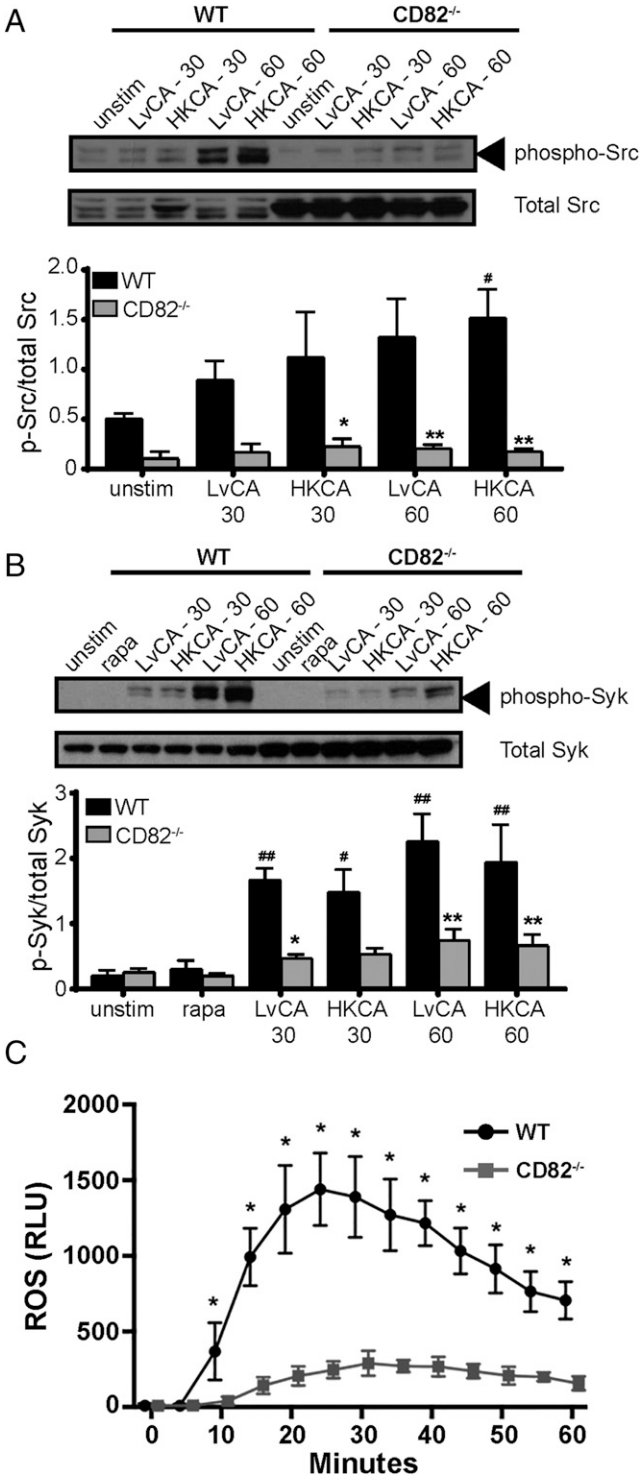

FIGURE 4. CD82 is required for downstream Dectin-1 signaling components. Phosphorylation of Src family kinases (**A**) and Syk (**B**), which occurs downstream of Dectin-1 activation, was elevated as soon as 30 min after stimulation with live and HKCA (LvCA and HKCA, respectively). Immunoblotting demonstrated reduced phosphorylation of both proteins in CD82$^{-/-}$ macrophages when compared with total Src or Syk. Quantification was performed using ImageJ software. (**C**) Ameliorated ROS generation was seen in CD82$^{-/-}$ macrophages (curve with squares) compared with WT (curve with circles) as measured by lucigenin assay. Src ($n = 3$); Syk ($n = 5$). $^{*}p < 0.05$, $^{**}p < 0.01$ versus WT. $^{\#}p < 0.05$, $^{\#\#}p < 0.01$ versus unstimulated.

individual Dectin-1 clusters can be distinguished (Supplemental Fig. 1B). Using STORM, we observed larger amounts of Dectin-1 clusters in the phagocytic cup in WT macrophages compared with CD82$^{-/-}$ macrophages (Fig. 6A). Quantitative analysis performed on these Dectin-1 clusters showed that, although cluster size was similar in both the WT and CD82$^{-/-}$ macrophages (Fig. 6B), fewer Dectin-1 clusters were seen in CD82$^{-/-}$ macrophages compared with WT macrophages (Fig. 6C). Based on these data, we conclude that CD82 organized Dectin-1 clustering in the phagocytic cup for downstream Dectin-1 signaling events.

Deletion of CD82 increases susceptibility to C. albicans *in mice*

To confirm the relevance of in vitro findings, we next investigated susceptibility of WT and CD82$^{-/-}$ mice to *C. albicans* bloodstream infection in an in vivo model of systemic candidiasis. Mice were i.v. infected with a lethal dose (1×10^5 yeast) of *C. albicans* and survival was monitored daily for 28 d. As expected, *C. albicans* challenge led to 100% mortality by day 8 in WT mice. On the contrary, mice lacking CD82 had significantly reduced survival, as seen by 100% mortality by day 6 postinfection (Fig. 7). These data demonstrate that the absence of CD82 leads to increase susceptibility to *C. albicans* infection.

CD82 polymorphisms affect Candida*-induced cytokine responses and candidemia susceptibility*

To test if CD82 is important for susceptibility to *Candida* infections in patients, we investigated CD82 polymorphisms for their association with *Candida*-induced cytokine production and susceptibility to candidemia. We identified two CD82 SNPs that affected IL-1β, IL-6, and IL-17 cytokine production after stimulation of human whole blood or PBMCs with *C. albicans*: rs12282890 and rs1429553 (Table I). Furthermore, the CD82 SNP rs7932712 was associated with an increased risk for candidemia but did not affect cytokine production. Overall, these polymorphisms indicate a key role for CD82 in human host defense and susceptibility to *Candida* infection.

Discussion

The data from the current study suggest a novel mechanism for Dectin-1 activation by *C. albicans* mediated by the tetraspanin CD82 (Fig. 8). The present study demonstrates that CD82 associates with Dectin-1 on the plasma membrane to organize Dectin-1 into TEMs in the phagocytic cup. Dectin-1 clustering via CD82 facilitates downstream Dectin-1 signaling, resulting in robust phosphorylation of Src family kinases and Syk as well as subsequent production of ROS. Additionally, deletion of CD82 in macrophages leads to reduced ROS production, cytokine production, and mRNA expression of TNF-α and IL-1β. Macrophages deficient in CD82 are less efficient at fungal killing and, therefore, there is higher replication within these macrophages. Furthermore, absence of CD82 in mice led to greater susceptibility to *C. albicans* as compared with CD82-proficient mice. We propose this mechanism serves to mediate antifungal immunity in macrophages.

Tetraspanins play a diverse range of functions through the interaction with membrane proteins (such as integrins, cadherins, and metalloproteinases) and intracellular vesicles (10, 13, 56). Indeed, a recent study showed an essential role of CD82 in cell-cell adhesion by downregulating Snail, an E-cadherin repressor, thereby suppressing metastasis in epithelial cancer cells (56). Not only are tetraspanins implicated in cancer, but they are also implicated in interactions with fungal pathogens. CD37 and CD63 have been shown to interact with fungal PRRs (36, 37), providing insight

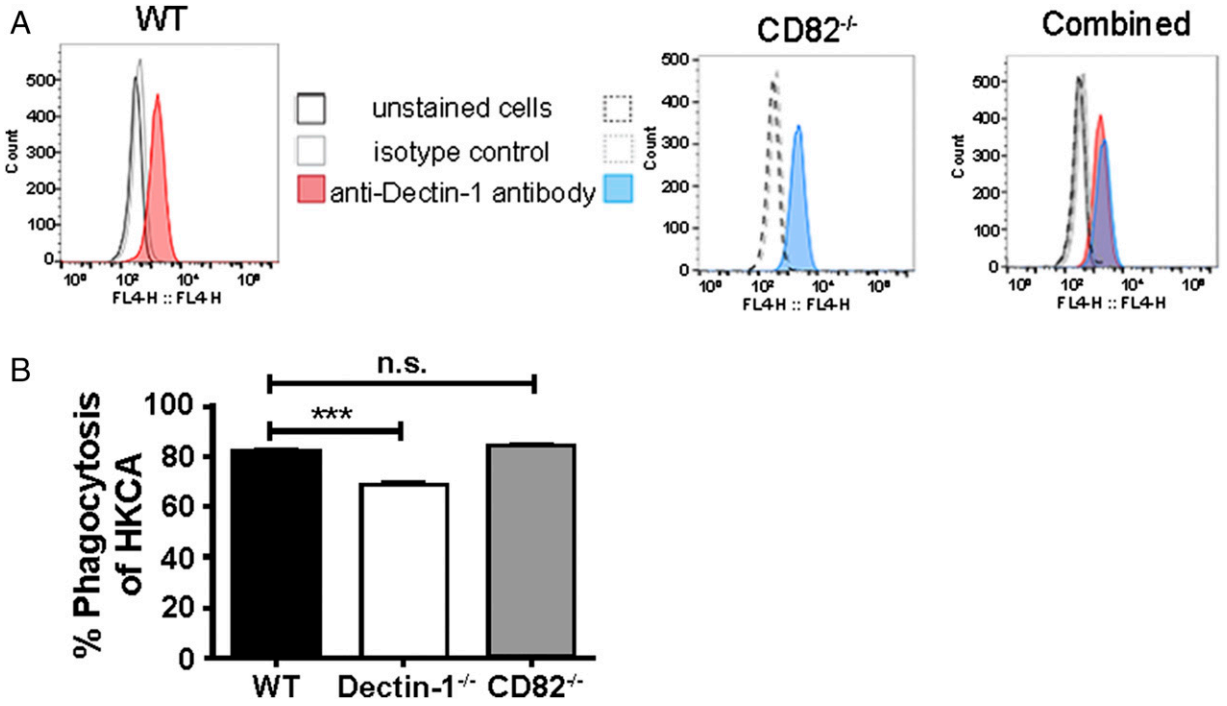

FIGURE 5. Macrophages lacking CD82 have no effect of Dectin-1 expression or phagocytosis. (**A**) Similar amounts of Dectin-1 expression were seen in WT (red) and CD82$^{-/-}$ (blue) macrophages as measured by flow cytometry using an anti–Dectin-1 Ab. Together, these peaks overlap in the third panel (purple). (**B**) No significant difference was observed in phagocytosis of HKCA between WT and CD82$^{-/-}$ macrophages. As a control, Dectin-1$^{-/-}$ primary macrophages were compared with WT. Dectin-1$^{-/-}$ macrophages had reduced phagocytosis of HKCA (n = 3). ***$p < 0.001$ versus WT.

into the organization of fungal PRR and downstream signaling. Additionally, recruitment of tetraspanins CD63 and CD82 have been reported to macrophage phagosomes containing fungi, such as *C. albicans, A. fumigatus,* and *C. neoformans* (24, 40). Although previous reports showed the kinetics of tetraspanin recruitment to the phagosome prior to acidification, there has been no insight into which fungal PRRs specifically associated with tetraspanins. This observation could be due to the complex composition of

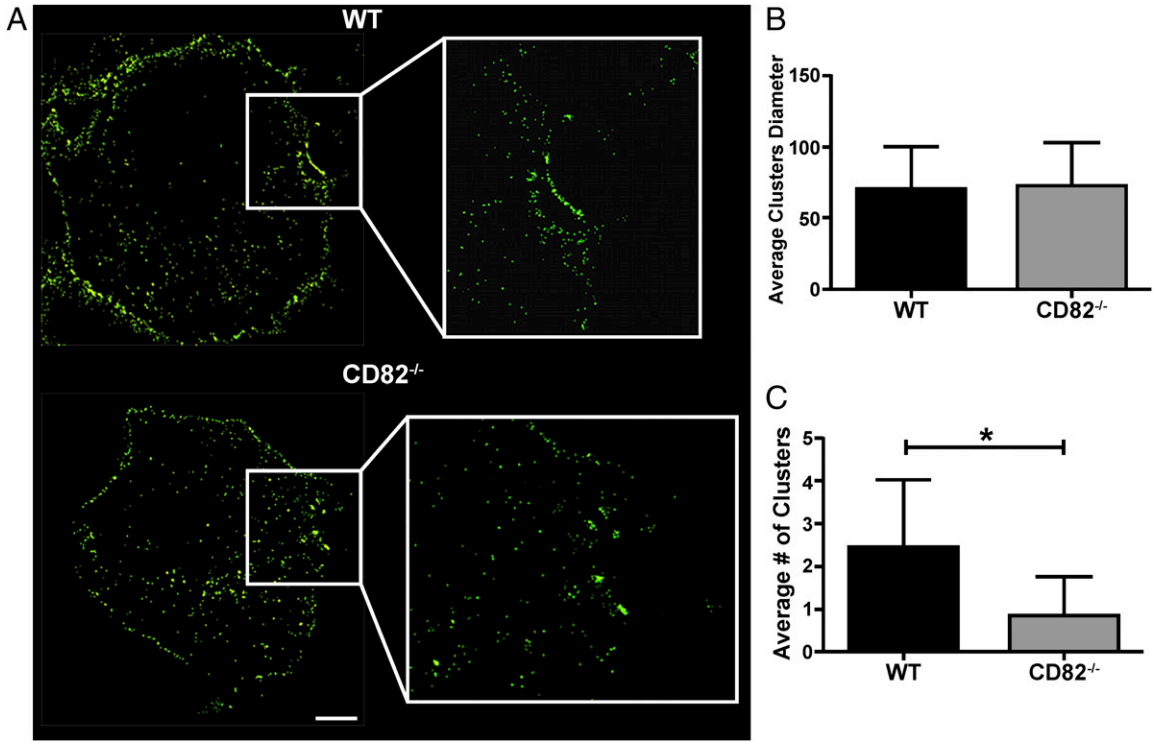

FIGURE 6. CD82 regulates Dectin-1 clustering in the phagocytic cup. (**A**) Macrophages were stimulated with HKCA for 15 min, then fixed using PFA. Lower panel, reduced Dectin-1 clustering was observed in CD82$^{-/-}$ macrophages compared with WT as seen by high-resolution STORM. Original magnification ×60. (**B**) Cluster size was not different between WT and CD82$^{-/-}$ macrophages. (**C**) In a cluster analysis of 20 cells, CD82$^{-/-}$ macrophages had fewer clusters compared with WT macrophages (n = 3). *$p < 0.05$ versus WT.

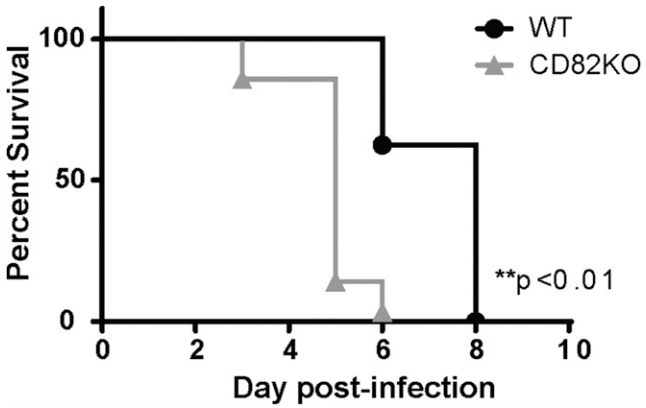

FIGURE 7. CD82 knockout mice are more susceptible to *C. albicans* infection. WT and CD82$^{-/-}$ mice were i.v. injected with *C. albicans* (1×10^5 CFU), and survival was monitored. The data are presented as Kaplan–Meier survival curves (WT $n = 8$; CD82$^{-/-}$ $n = 7$).

carbohydrates and proteins on the surface of the fungal cell wall (34). Because of the heterogenous composition of the fungal cell wall, it has been difficult to dissect specific associations between fungal PRRs, tetraspanins, and other proteins. To address this problem, we used FLPs coated with discrete, purified fungal carbohydrates (57) to perform proteomic analyses and observed tetraspanin CD82 associated with both β-1,3-glucan and mannan FLPs. These results implicate a specific association with Dectin-1 and CD82.

The association between CD82 and Dectin-1 was further confirmed by co-IP, fluorescent microscopy, phagosome isolation, and PLA. In our co-IP studies, association between CD82 and Dectin-1 is only seen using Brij 58 lysis buffer, a mild detergent, thereby classifying the nature of CD82–Dectin-1 interaction as indirect. Although an association was observed in resting macrophages using co-IP, we did not observe an association between CD82 and Dectin-1 on the plasma membrane of resting cells using PLA. This difference could be due to the interaction between CD82 and Dectin-1 is greater than the theoretical maximum distance of 30–40 nm to create a signal with PLA (58). CD82 has been shown to interact with other membrane proteins, including CD63 and class II MHC (40). Furthermore, it has been well demonstrated that tetraspanins interact with each other as well as other transmembrane proteins (i.e., integrins, Ig, receptors for cytokines and growth factors, etc.) (9, 10, 13, 59). CD82 may act indirectly through these other protein interactions to facilitate Dectin-1 signaling at the phagocytic cup. Indeed, Dectin-1 has been shown to interact with the tetraspanins CD63 (36) and CD37 (37, 38). Deletion of CD37 resulted in reduced Dectin-1 cell surface localization (37). Further investigation into CD82–Dectin-1 interaction with other transmembrane or tetraspanin proteins is warranted. In many conditions, loss of a single tetraspanin fails to reveal a specific phenotype. However, our studies revealed a nonredundant role of CD82 in Dectin-1–mediated signaling in macrophages.

Because CD82 creates signaling domains on the plasma membrane and association between CD82 and Dectin-1 was corroborated using several techniques, we next examined the consequences of CD82 deletion on Dectin-1 and associated clustering. In order for Dectin-1 to signal properly, it must cluster in the phagocytic synapse through particulate binding of an organism containing β-1,3-glucan (33). Without Dectin-1 clustering, cells have decreased Syk phosphorylation and ROS generation. Although we were unable to investigate individual Dectin-1 clusters using traditional epifluorescence techniques, use of the superresolution technique STORM showed that CD82 mediates Dectin-1 clustering in the phagocytic synapse for Src and Syk phosphorylation and ROS production. Taken together, these techniques demonstrate an interaction between CD82 and Dectin-1 on the phagosome. Deletion of CD82 from macrophages reduced Dectin-1 signaling events and, in turn, increased fungal burden within macrophages. Tetraspanins are implicated in a variety of membrane organization-related processes; therefore, future studies should investigate changes in sensitivity to membrane stressors in CD82-deficient cells (10, 13). Although the cardiovascular system, eye, bone, and metabolism are impacted with deletion of CD82, mice are viable and have no physiological abnormalities (60–63). Therefore, to demonstrate the relevance of our in vitro findings, we used an in vivo model of systemic candidiasis to show that mice lacking CD82 have enhanced susceptibility to *Candida* compared with WT mice. Furthermore, by incorporating human data, we show that human polymorphisms in CD82 result in modifications of cytokine production and increased susceptibility to candidemia. These data provide critical insight and a novel therapeutic target for the prevention and treatment of *Candida* infections.

In this study, a novel interaction between tetraspanin CD82 and Dectin-1 was identified. We also show the role of CD82 in the organization of Dectin-1 clustering in the phagocytic cup. Deletion of CD82 disrupts macrophage response to fungal pathogens, such as *C. albicans,* leading to increased fungal viability and decreased host survival. In support of this hypothesis, we see higher metabolism of *C. albicans* and higher

Table I. List of CD82 SNPs associated with cytokine changes and candidemia susceptibility

SNPs	eQTL[a] *p* Value	Cytokine Affected	Affected Sample	cQTL[b] *p* Value	Candidemia Susceptibility *p* Value	Risk Allele Frequency	Candidemia Susceptibility Odds Ratio
rs12282890	6.22×10^{-06}	IL-1β	*Candida* blastospores, (HKCA), WB, 48 h	0.0122	NS[c]	n/a	n/a
rs12282890	6.22×10^{-06}	IL-17	*C. albicans* blastospores, PBMC, 7 d	0.0471	NS[c]	n/a	n/a
rs1429553	1.11×10^{-03}	IL-6	*C. albicans* hyphae, PBMC, 24 h	0.0018	NS[c]	n/a	n/a
rs7932712	0.0014	None	n/a	NS[c]	0.0215	C, 0.71	1.49

List of CD82 SNPs in the 500 Functional Genomics Project cohort for *Candida*-induced cytokines and candidemia susceptibility in WB or PBMC samples. Two polymorphisms were associated with changes to IL-1β, IL-17, and IL-6 cytokines. The SNP rs7932712 was associated with an elevated susceptibility to develop candidemia.
[a]SNPs correlated with expression level of CD82 SNPs were tested but are not associated with the phenotype.
[b]SNPs correlated with cytokine levels.
[c]SNPs were tested but are not associated with the phenotype.
cQTL, cytokine quantitative trait locus; eQTL, expression quantitative trait locus; WB, whole blood.

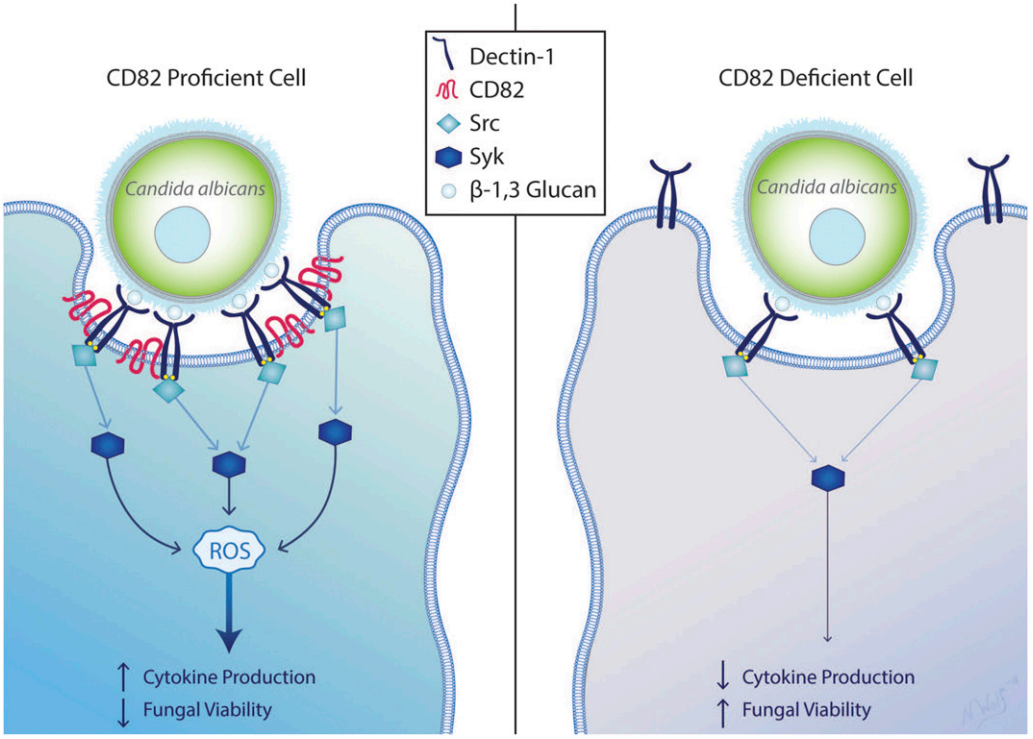

FIGURE 8. Schematic representation of CD82 and Dectin-1 interaction after *C. albicans* activation. In CD82-proficient cells, Dectin-1 is activated by β-1,3 glucan on the cell wall of *C. albicans*. Subsequent activation of Src, then Syk, leads to production of ROS, elevated cytokines, and reduction in fungal viability. Presence of CD82 contributes to Dectin-1 molecular organization in the membrane. Cells lacking CD82 have reduced Dectin-1 clustering in the phagocytic cup, which contributes to reduced Syk phosphorylation, ROS, and cytokine production. CD82-deficiency leads to higher fungal burden. Illustration by Nicole Wolf, MS, ©2018. Printed with permission.

CFU in macrophages. Interestingly, we observed multiple CD82 SNPs in whole blood or PBMC from patients associated with modulation of cytokine production or increased risk of *Candida* infections. From these findings, we suggest CD82 as a potential new target in modulating the host response to fungal pathogens, including *C. albicans,* whereby deletion of CD82 reduces the inflammatory response to the pathogen. These results add to the body of literature that illustrates the growing role of tetraspanins in the interaction between the host and fungal pathogens.

Acknowledgments

We thank Dr. Gordon Brown, Dr. Douglas Golenbock, and Dr. Stuart Levitz for reagents and Nicole Wolf for assistance with the artwork (illustration [Fig. 8/visual abstract] by Nicole Wolf, MS, ©2018). Printed with permission. We also thank Hazen Babcock for useful discussions in image analysis for STORM.

Disclosures

The authors have no financial conflicts of interest.

References

1. Menzin, J., J. L. Meyers, M. Friedman, J. R. Korn, J. R. Perfect, A. A. Langston, R. P. Danna, and G. Papadopoulos. 2011. The economic costs to United States hospitals of invasive fungal infections in transplant patients. *Am. J. Infect. Control* 39: e15–e20.
2. Miceli, M. H., J. A. Díaz, and S. A. Lee. 2011. Emerging opportunistic yeast infections. *Lancet Infect. Dis.* 11: 142–151.
3. Lanternier, F., S. Cypowyj, C. Picard, J. Bustamante, O. Lortholary, J. L. Casanova, and A. Puel. 2013. Primary immunodeficiencies underlying fungal infections. *Curr. Opin. Pediatr.* 25: 736–747.
4. Calderone, R. A., and W. A. Fonzi. 2001. Virulence factors of *Candida albicans*. *Trends Microbiol.* 9: 327–335.
5. Nobile, C. J., and A. D. Johnson. 2015. *Candida albicans* biofilms and human disease. *Annu. Rev. Microbiol.* 69: 71–92.
6. Pfaller, M. A., and M. Castanheira. 2016. Nosocomial candidiasis: antifungal stewardship and the importance of rapid diagnosis. *Med. Mycol.* 54: 1–22.
7. Pfaller, M. A., and D. J. Diekema. 2010. Epidemiology of invasive mycoses in North America. *Crit. Rev. Microbiol.* 36: 1–53.
8. van Spriel, A. B., and C. G. Figdor. 2010. The role of tetraspanins in the pathogenesis of infectious diseases. *Microbes Infect.* 12: 106–112.
9. Charrin, S., S. Jouannet, C. Boucheix, and E. Rubinstein. 2014. Tetraspanins at a glance. *J. Cell Sci.* 127: 3641–3648.
10. Charrin, S., F. le Naour, O. Silvie, P.-E. Milhiet, C. Boucheix, and E. Rubinstein. 2009. Lateral organization of membrane proteins: tetraspanins spin their web. *Biochem. J.* 420: 133–154.
11. Yang, X., C. Claas, S. K. Kraeft, L. B. Chen, Z. Wang, J. A. Kreidberg, and M. E. Hemler. 2002. Palmitoylation of tetraspanin proteins: modulation of CD151 lateral interactions, subcellular distribution, and integrin-dependent cell morphology. *Mol. Biol. Cell* 13: 767–781.
12. Berditchevski, F., E. Odintsova, S. Sawada, and E. Gilbert. 2002. Expression of the palmitoylation-deficient CD151 weakens the association of alpha 3 beta 1 integrin with the tetraspanin-enriched microdomains and affects integrin-dependent signaling. *J. Biol. Chem.* 277: 36991–37000.
13. Yáñez-Mó, M., O. Barreiro, M. Gordon-Alonso, M. Sala-Valdés, and F. Sánchez-Madrid. 2009. Tetraspanin-enriched microdomains: a functional unit in cell plasma membranes. *Trends Cell Biol.* 19: 434–446.
14. Dong, J. T., P. W. Lamb, C. W. Rinker-Schaeffer, J. Vukanovic, T. Ichikawa, J. T. Isaacs, and J. C. Barrett. 1995. KAI1, a metastasis suppressor gene for prostate cancer on human chromosome 11p11.2. *Science* 268: 884–886.
15. Iwata, S., H. Kobayashi, R. Miyake-Nishijima, T. Sasaki, A. Souta-Kuribara, M. Nori, O. Hosono, H. Kawasaki, H. Tanaka, and C. Morimoto. 2002. Distinctive signaling pathways through CD82 and beta1 integrins in human T cells. *Eur. J. Immunol.* 32: 1328–1337.
16. Wu, Q., Y. Yang, S. Wu, W. Li, N. Zhang, X. Dong, and Y. Ou. 2015. Evaluation of the correlation of KAI1/CD82, CD44, MMP7 and β-catenin in the prediction of prognosis and metastasis in colorectal carcinoma. *Diagn. Pathol.* 10: 176.
17. Adachi, M., T. Taki, Y. Ieki, C. L. Huang, M. Higashiyama, and M. Miyake. 1996. Correlation of KAI1/CD82 gene expression with good prognosis in patients with non-small cell lung cancer. *Cancer Res.* 56: 1751–1755.
18. Sho, M., M. Adachi, T. Taki, H. Hashida, T. Konishi, C. L. Huang, N. Ikeda, Y. Nakajima, H. Kanehiro, M. Hisanaga, et al. 1998. Transmembrane 4 superfamily as a prognostic factor in pancreatic cancer. *Int. J. Cancer* 79: 509–516.
19. Huang, C. I., N. Kohno, E. Ogawa, M. Adachi, T. Taki, and M. Miyake. 1998. Correlation of reduction in MRP-1/CD9 and KAI1/CD82 expression with recurrences in breast cancer patients. *Am. J. Pathol.* 153: 973–983.
20. Houle, C. D., X. Y. Ding, J. F. Foley, C. A. Afshari, J. C. Barrett, and B. J. Davis. 2002. Loss of expression and altered localization of KAI1 and CD9 protein are

associated with epithelial ovarian cancer progression. *Gynecol. Oncol.* 86: 69–78.
21. Kropshofer, H., S. Spindeldreher, T. A. Röhn, N. Platania, C. Grygar, N. Daniel, A. Wölpl, H. Langen, V. Horejsi, and A. B. Vogt. 2002. Tetraspan microdomains distinct from lipid rafts enrich select peptide-MHC class II complexes. *Nat. Immunol.* 3: 61–68.
22. Hammond, C., L. K. Denzin, M. Pan, J. M. Griffith, H. J. Geuze, and P. Cresswell. 1998. The tetraspan protein CD82 is a resident of MHC class II compartments where it associates with HLA-DR, -DM, and -DO molecules. *J. Immunol.* 161: 3282–3291.
23. Poloso, N. J., L. K. Denzin, and P. A. Roche. 2006. CDw78 defines MHC class II-peptide complexes that require Ii chain-dependent lysosomal trafficking, not localization to a specific tetraspanin membrane microdomain. *J. Immunol.* 177: 5451–5458.
24. Artavanis-Tsakonas, K., P. V. Kasperkovitz, E. Papa, M. L. Cardenas, N. S. Khan, A. G. Van der Veen, H. L. Ploegh, and J. M. Vyas. 2011. The tetraspanin CD82 is specifically recruited to fungal and bacterial phagosomes prior to acidification. *Infect. Immun.* 79: 1098–1106.
25. Brown, G. D., and S. Gordon. 2001. Immune recognition. A new receptor for beta-glucans. *Nature* 413: 36–37.
26. Saijo, S., N. Fujikado, T. Furuta, S. H. Chung, H. Kotaki, K. Seki, K. Sudo, S. Akira, Y. Adachi, N. Ohno, et al. 2007. Dectin-1 is required for host defense against *Pneumocystis carinii* but not against *Candida albicans*. *Nat. Immunol.* 8: 39–46.
27. Sancho, D., and C. Reis e Sousa. 2012. Signaling by myeloid C-type lectin receptors in immunity and homeostasis. *Annu. Rev. Immunol.* 30: 491–529.
28. Netea, M. G., and L. Maródi. 2010. Innate immune mechanisms for recognition and uptake of Candida species. *Trends Immunol.* 31: 346–353.
29. Cunha, C., M. Di Ianni, S. Bozza, G. Giovannini, S. Zagarella, T. Zelante, C. D'Angelo, A. Pierini, L. Pitzurra, F. Falzetti, et al. 2010. Dectin-1 Y238X polymorphism associates with susceptibility to invasive aspergillosis in hematopoietic transplantation through impairment of both recipient- and donor-dependent mechanisms of antifungal immunity. *Blood* 116: 5394–5402.
30. Ferwerda, B., G. Ferwerda, T. S. Plantinga, J. A. Willment, A. B. van Spriel, H. Venselaar, C. C. Elbers, M. D. Johnson, A. Cambi, C. Huysamen, et al. 2009. Human dectin-1 deficiency and mucocutaneous fungal infections. *N. Engl. J. Med.* 361: 1760–1767.
31. Goodridge, H. S., T. Shimada, A. J. Wolf, Y. M. Hsu, C. A. Becker, X. Lin, and D. M. Underhill. 2009. Differential use of CARD9 by dectin-1 in macrophages and dendritic cells. *J. Immunol.* 182: 1146–1154.
32. Rogers, N. C., E. C. Slack, A. D. Edwards, M. A. Nolte, O. Schulz, E. Schweighoffer, D. L. Williams, S. Gordon, V. L. Tybulewicz, G. D. Brown, and C. Reis e Sousa. 2005. Syk-dependent cytokine induction by Dectin-1 reveals a novel pattern recognition pathway for C type lectins. *Immunity* 22: 507–517.
33. Goodridge, H. S., C. N. Reyes, C. A. Becker, T. R. Katsumoto, J. Ma, A. J. Wolf, N. Bose, A. S. Chan, A. S. Magee, M. E. Danielson, et al. 2011. Activation of the innate immune receptor Dectin-1 upon formation of a 'phagocytic synapse'. *Nature* 472: 471–475.
34. Underhill, D. M., E. Rossnagle, C. A. Lowell, and R. M. Simmons. 2005. Dectin-1 activates Syk tyrosine kinase in a dynamic subset of macrophages for reactive oxygen production. *Blood* 106: 2543–2550.
35. Drummond, R. A., S. Saijo, Y. Iwakura, and G. D. Brown. 2011. The role of Syk/CARD9 coupled C-type lectins in antifungal immunity. *Eur. J. Immunol.* 41: 276–281.
36. Mantegazza, A. R., M. M. Barrio, S. Moutel, L. Bover, M. Weck, P. Brossart, J. L. Teillaud, and J. Mordoh. 2004. CD63 tetraspanin slows down cell migration and translocates to the endosomal-lysosomal-MIICs route after extracellular stimuli in human immature dendritic cells. *Blood* 104: 1183–1190.
37. Meyer-Wentrup, F., C. G. Figdor, M. Ansems, P. Brossart, M. D. Wright, G. J. Adema, and A. B. van Spriel. 2007. Dectin-1 interaction with tetraspanin CD37 inhibits IL-6 production. *J. Immunol.* 178: 154–162.
38. van Spriel, A. B., M. Sofi, K. H. Gartlan, A. van der Schaaf, I. Verschueren, R. Torensma, R. A. Raymakers, B. E. Loveland, M. G. Netea, G. J. Adema, et al. 2009. The tetraspanin protein CD37 regulates IgA responses and anti-fungal immunity. *PLoS Pathog.* 5: e1000338.
39. Hornung, V., F. Bauernfeind, A. Halle, E. O. Samstad, H. Kono, K. L. Rock, K. A. Fitzgerald, and E. Latz. 2008. Silica crystals and aluminum salts activate the NALP3 inflammasome through phagosomal destabilization. *Nat. Immunol.* 9: 847–856.
40. Artavanis-Tsakonas, K., J. C. Love, H. L. Ploegh, and J. M. Vyas. 2006. Recruitment of CD63 to *Cryptococcus neoformans* phagosomes requires acidification. *Proc. Natl. Acad. Sci. USA* 103: 15945–15950.
41. Mansour, M. K., J. M. Tam, N. S. Khan, M. Seward, P. J. Davids, S. Puranam, A. Sokolovska, D. B. Sykes, Z. Dagher, C. Becker, et al. 2013. Dectin-1 activation controls maturation of β-1,3-glucan-containing phagosomes. *J. Biol. Chem.* 288: 16043–16054.
42. Bagag, A., J. M. Jault, N. Sidahmed-Adrar, M. Réfrégiers, A. Giuliani, and F. Le Naour. 2013. Characterization of hydrophobic peptides in the presence of detergent by photoionization mass spectrometry. *PLoS One* 8: e79033.
43. Bagag, A., A. Giuliani, F. Canon, M. Réfrégiers, and F. Le Naour. 2011. Separation of peptides from detergents using ion mobility spectrometry. *Rapid Commun. Mass Spectrom.* 25: 3436–3440.
44. Bates, M., S. A. Jones, and X. Zhuang. 2013. Stochastic optical reconstruction microscopy (STORM): a method for superresolution fluorescence imaging. *Cold Spring Harb. Protoc.* 2013: 498–520.
45. Levet, F., E. Hosy, A. Kechkar, C. Butler, A. Beghin, D. Choquet, and J. B. Sibarita. 2015. SR-Tesseler: a method to segment and quantify localization-based super-resolution microscopy data. *Nat. Methods* 12: 1065–1071.
46. Li, Y., M. Oosting, S. P. Smeekens, M. Jaeger, R. Aguirre-Gamboa, K. T. T. Le, P. Deelen, I. Ricaño-Ponce, T. Schoffelen, A. F. M. Jansen, et al. 2016. A functional genomics approach to understand variation in cytokine production in humans. *Cell* 167: 1099–1110.e14.
47. Ward, L. D., and M. Kellis. 2012. HaploReg: a resource for exploring chromatin states, conservation, and regulatory motif alterations within sets of genetically linked variants. *Nucleic Acids Res.* 40(Database issue): D930–D934.
48. Kumar, V., S. C. Cheng, M. D. Johnson, S. P. Smeekens, A. Wojtowicz, E. Giamarellos-Bourboulis, J. Karjalainen, L. Franke, S. Withoff, T. S. Plantinga, et al. 2014. Immunochip SNP array identifies novel genetic variants conferring susceptibility to candidaemia. *Nat. Commun.* 5: 4675.
49. Matzaraki, V., M. S. Gresnigt, M. Jaeger, I. Ricaño-Ponce, M. D. Johnson, M. Oosting, L. Franke, S. Withoff, J. R. Perfect, L. A. B. Joosten, et al. 2017. An integrative genomics approach identifies novel pathways that influence candidaemia susceptibility. *PLoS One* 12: e0180824.
50. Tam, J. M., M. K. Mansour, N. S. Khan, M. Seward, S. Puranam, A. Tanne, A. Sokolovska, C. E. Becker, M. Acharya, M. A. Baird, et al. 2014. Dectin-1-dependent LC3 recruitment to phagosomes enhances fungicidal activity in macrophages. *J. Infect. Dis.* 210: 1844–1854.
51. Stuart, L. M., J. Boulais, G. M. Charriere, E. J. Hennessy, S. Brunet, I. Jutras, G. Goyette, C. Rondeau, S. Letarte, H. Huang, et al. 2007. A systems biology analysis of the Drosophila phagosome. *Nature* 445: 95–101.
52. Claas, C., C. S. Stipp, and M. E. Hemler. 2001. Evaluation of prototype transmembrane 4 superfamily protein complexes and their relation to lipid rafts. *J. Biol. Chem.* 276: 7974–7984.
53. Schuck, S., M. Honsho, K. Ekroos, A. Shevchenko, and K. Simons. 2003. Resistance of cell membranes to different detergents. *Proc. Natl. Acad. Sci. USA* 100: 5795–5800.
54. Wheeler, R. T., and G. R. Fink. 2006. A drug-sensitive genetic network masks fungi from the immune system. *PLoS Pathog.* 2: e35.
55. Bagchi, S., R. Fredriksson, and Å. Wallén-Mackenzie. 2015. In situ proximity ligation assay (PLA). *Methods Mol. Biol.* 1318: 149–159.
56. Lee, M. S., H. J. Byun, J. Lee, D. I. Jeoung, Y. M. Kim, and H. Lee. 2018. Tetraspanin CD82 represses Sp1-mediated Snail expression and the resultant E-cadherin expression interrupts nuclear signaling of β-catenin by increasing its membrane localization. *Cell. Signal.* 52: 83–94.
57. Tam, J. M., M. K. Mansour, N. S. Khan, N. C. Yoder, and J. M. Vyas. 2012. Use of fungal derived polysaccharide-conjugated particles to probe Dectin-1 responses in innate immunity. *Integr. Biol. (Camb)* 4: 220–227.
58. Söderberg, O., M. Gullberg, M. Jarvius, K. Ridderstråle, K. J. Leuchowius, J. Jarvius, K. Wester, P. Hydbring, F. Bahram, L. G. Larsson, and U. Landegren. 2006. Direct observation of individual endogenous protein complexes in situ by proximity ligation. *Nat. Methods* 3: 995–1000.
59. Boucheix, C., and E. Rubinstein. 2001. Tetraspanins. *Cell. Mol. Life Sci.* 58: 1189–1205.
60. Risinger, J. I., M. Custer, L. Feigenbaum, R. M. Simpson, S. B. Hoover, J. D. Webster, G. V. Chandramouli, L. Tessarollo, and J. C. Barrett. 2014. Normal viability of Kai1/Cd82 deficient mice. *Mol. Carcinog.* 53: 610–624.
61. Wei, Q., F. Zhang, M. M. Richardson, N. H. Roy, W. Rodgers, Y. Liu, W. Zhao, C. Fu, Y. Ding, C. Huang, et al. 2014. CD82 restrains pathological angiogenesis by altering lipid raft clustering and CD44 trafficking in endothelial cells. *Circulation* 130: 1493–1504.
62. Uchtmann, K., E. R. Park, A. Bergsma, J. Segula, M. J. Edick, and C. K. Miranti. 2015. Homozygous loss of mouse tetraspanin CD82 enhances integrin αIIbβ3 expression and clot retraction in platelets. *Exp. Cell Res.* 339: 261–269.
63. Bergsma, A., S. S. Ganguly, D. Dick, B. O. Williams, and C. K. Miranti. 2018. Global deletion of tetraspanin CD82 attenuates bone growth and enhances bone marrow adipogenesis. *Bone* 113: 105–113.